PNAS
www.pnas.org

Supplementary Information for

Mic60 exhibits a coordinated clustered distribution along and across yeast and mammalian mitochondria

Stefan Stoldt[a,1], Till Stephan[a,1], Daniel C. Jans[b,c], Christian Brüser[a], Felix Lange[a], Jan Keller-Findeisen[a], Dietmar Riedel[d], Stefan W. Hell[a], and Stefan Jakobs[a,b,2]

[1]S.S. and T.S. contributed equally to this work

[2]To whom correspondence may be adressed. Email: sjakobs@gwdg.de

This PDF file includes:

SI Materials and Methods
Figs. S1 to S4
Tables S1 to S4
Captions for movies S1 and S2
References for SI reference citations

Other supplementary materials for this manuscript include the following:

Movies S1 and S2

SI Materials and Methods

Yeast strains, genomic tagging and growth conditions

For the analysis of sub-mitochondrial protein distributions in the yeast *Saccharomyces cerevisiae* either GFP fusion strains from the Yeast GFP Clone Collection (BY4741; Cat. No.: 95702, Invitrogen, Carlsbad, CA, USA) or newly tagged strains isogenic to the wild type strain W303 were utilized. Genomic tagging to generate GFP fusions of the proteins of interest was achieved by directed homologous recombination of a PCR product using a *HIS3* cassette for positive selection as described previously (36) (Table S1 and S2). A TEV protease specific cleavage site was introduced between the linker and the EGFP sequence of pYM28 (37) to generate the pYM28-spacer-TEV-GFP template plasmid for genomic tagging. All epitope tagged strains were verified by PCR. Only yeast strains expressing full-length GFP fusion proteins and showing normal growth on a non-fermentable carbon source were used for this study. For targeted gene disruption of *MIC10* a PCR fragment was generated using genomic DNA isolated from a *Δmic10::kanMX4* strain (Table S1 and S3). The gene disruption was performed as described previously (36). Cultivation of yeast cells was performed according to standard protocols on agar plates or in liquid medium containing 2 % (w/v) glucose or 2 % (w/v) galactose, respectively.

Immunofluorescence labelling of yeast cells

Yeast cells were grown to the early exponential growth phase ($OD_{600\ nm}$ = 0.4 - 0.7) in liquid medium containing 2 % galactose as the sole carbon source. The cells were fixed with 3.7 % formaldehyde in the growth medium at room temperature (RT, 20 min), spun down (800 x *g*, 3 min) and washed with phosphate buffered saline with sorbitol (PBS/sorbitol) (137 mM NaCl; 3 mM KCl; 8 mM Na_2HPO_4; 1.5 mM KH_2PO_4; 10 % (w/v) sorbitol; pH 7). Afterwards, cell walls were partially removed by zymolyase treatment (15 min, 30 °C). Subsequently, the cells were washed with PBS/sorbitol. Cells were bound to the surface of poly-L-lysine coated cover slips (RT, 30 min) and blocked with a blocking solution containing 2 % (w/v) bovine serum albumin (BSA), 0,4 % (w/v) SDS, 0.1 % (v/v) Tween20 in PBS/sorbitol (RT, 60 min). Detection of specific epitopes was achieved by incubation of the samples with primary antibodies (4 °C, overnight; Table S4). Following

two further washing steps with blocking solution, cells were decorated with secondary antibodies custom-labeled with Abberior STAR RED (Abberior, Göttingen, Germany) or Alexa Fluor 594 (Thermo Fisher Scientific, Waltham, MA, USA) (RT, 90 min). After several additional washing steps in blocking solution and PBS/sorbitol, the samples were mounted in Mowiol containing 1,4-Diazabicyclo[2.2.2]octan (DABCO). For all antibodies see Table S4.

Cell culture and immunofluorescence staining of human primary dermal fibroblasts and human kidney carcinoma cells

Human kidney carcinoma cells (A-498) were cultured in DMEM, high glucose, pyruvate (Thermo Fisher Scientific) supplemented with Penicillin-Streptomycin (Sigma Aldrich, St. Louis, MO, USA) and 10 % (v/v) fetal bovine serum (Thermo Fisher Scientific).

Human primary dermal fibroblasts (HDFa, ATCC, Manassas, VA, USA) were cultured in DMEM containing 4,5 g/L Glucose and GlutaMAX™ additive (Thermo Fisher Scientific) supplemented with 100 U/ml penicillin and 100 µg/mL streptomycin (Merck Millipore, Burlington, MA, USA), 1mM sodium pyruvate (Sigma Aldrich) and 10 % (v/v) fetal bovine serum (Merck Millipore).

Cells were seeded on coverslips and cultured for 1-3 days (37 °C, 5 % CO_2). For immunolabeling, cells were fixed with a pre-warmed solution of 4 % formaldehyde in PBS (137 mM NaCl, 2.68 mM KCl and 10 mM Na_2HPO_4 , pH 7.4) (37 °C, 5 min).

Cells were extracted with 0.5 % (v/v) Triton X-100 in PBS and afterwards blocked with 5% (w/v) BSA in PBS/Glycine (0.1 M) (RT, 10 min). Mic60 was labeled using primary antibodies specific for Mic60/IMMT (Proteintech, Rosemont, IL, USA). HDFas were labeled for Tom22 with specific primary antibodies (Miltenyi Biotec, Bergisch Gladbach, Germany). A-498 cells were labeled for Tom20 using a mixture of different primary antibodies against Tom20 (Santa Cruz Biotechnology, Dallas, TX, USA and Abcam, Cambridge, UK). The primary antibodies were diluted in 5 % BSA (w/v) in PBS/Glycine (0.1 M) and applied to the samples (RT, 1h). After five washing steps with PBS and blocking with 5 % BSA in PBS/Glycine (0.1 M), the primary antibodies were detected with secondary goat anti-rabbit or sheep anti-mouse antibodies (Jackson Immuno Research Laboratories, West Grove, PA, USA) custom-labeled with Abberior STAR RED

(Abberior) or Alexa Fluor 594 (Thermo Fisher Scientific) or secondary goat antibodies labeled with Alexa Fluor 555 (Abcam) (RT, 1h). The samples were washed five times with PBS and mounted in Mowiol mounting medium containing 0.1 % (w/v) DABCO (Sigma Aldrich). For all antibodies see Table S4.

2D STED nanoscopy

2D STED nanoscopy was performed using a 775 nm quad scanning STED microscope (Abberior Instruments, Göttingen, Germany) equipped with a UPlanSApo 100x/1,40 Oil objective (Olympus, Tokyo, Japan) and a Katana-08 HP laser (Onefive GmbH, Regensdorf, Switzerland) utilizing a pixel size of 15 nm. The fluorophore Alexa Fluor 594 was excited at 594 nm, Abberior STAR RED was excited at 640 nm and STED was performed at 775 nm wavelength. 2D STED data were linearly deconvolved using the Imspector software (Abberior Instruments).

3D STED nanoscopy

3D STED nanoscopy was performed on a Leica TCS SP8 STED 3X (Leica Microsystems, Wetzlar, Germany) equipped with a HC PL APO 100X/1.40 Oil STED WHITE objective. The fluorophore Alexa Fluor 555 was excited at 521 nm and STED was performed at 660 nm. The 3D STED data were deconvolved using Huygens deconvolution software (Scientific Volume Imaging, Hilversum, Netherlands) and rendered (volume rendition) and animated using Imaris (Bitplane, Zurich, Switzerland).

Quantification of twisted and parallel distribution bands

To quantify the occurrence of different Mic60 distribution patterns in HDFa cells, STED recordings were manually analyzed. Three categories for the analysis were pre-defined: ‘twisted bands’, ‘parallel bands’ and ‘not assigned’. On the STED images, all mitochondrial tubules were independently assigned by three test persons to one of the three categories. Contiguous mitochondrial tubules could consist out of sections assigned to different categories. No specifications were given for the length of the mitochondrial sections that were assigned. The total length of mitochondrial tubules assigned to the

different categories were analyzed by a computer program and the relative amount of the different categories with respect to the length of the entire network were determined.

Averaging of 3D sections of straightened mitochondria imaged with 3D STED microscopy

Recorded 3D STED data stacks with a pixel size of 22.5 nm x 22.5 nm x 40 nm were deconvolved with a 3D Gaussian peak function of 150 nm FWHM in all directions applying the Richardson-Lucy algorithm for 20 iterations. Then they were visually inspected and single, straight sections of the mitochondrial network were cut out. Further processing was performed with a custom written script in Matlab (Mathworks, Natick, USA). First, the present section of the mitochondrial network was rotated to be parallel with the x-axis of the coordinate system by visually determining a rotation angle in the xy plane. Correcting the mitochondrial tube for a shift along the z-axis was also possible, but the chosen rotation angles in the yz plane were typically < 1°. A linear 3D interpolation on a rotated grid of cubic pixels with a size of 10 nm resulted in the mitochondrial section being parallel with the x-axis and only slightly bended. The section was further straightened by binning slices 10 times along the x direction and correlating the binned slices with each other. The maximum of this 2D correlation gave rise to a shift in the yz plane that could be applied inversely to stack the mitochondrial slices along the x direction without any residual systematic bend. A desired length of the straightened 3D section of mitochondria could then be added up.

For Fig. S3, the straightened tubules were automatically segmented into sections of 1.5 µm, each overlapping with the next by 750 nm. Subsequently, the fluorescence signal of each section along the longitudinal mitochondrial axis (over 1.5 µm) was added up. All added-up sections were manually assigned to different categories.

Cluster and correlation analysis of 2D sections of straightened mitochondria imaged with 2D STED microscopy

The recorded 2D STED data had a pixel size of 15 nm x 15 nm. Data analysis was performed using custom written Matlab scripts.

First, rectangular regions of interest (ROI) were determined by visually inspecting the 2D images. The ROI rectangle could be rotated and the rotation was chosen so that the interesting section of the mitochondrial network was mostly parallel to one border of the rectangle.

In a next step, the centerline of the section of mitochondria in each ROI was determined. This was performed by smoothing the image with an asymmetrical 2D Gaussian peak function of 500 nm FWHM longitudinally along the mitochondria and 100 nm FWHM across. A line detection algorithm, detecting lines of local maxima could reliably detect the centerline of mitochondria on the smoothed data. The centerline itself was also quite smooth.

A perpendicular grid was placed around that centerline by calculating lines vertical to the center line in regular distances (10 nm) and placing grid points in regular distances (10 nm) on these vertical lines. A linear 2D interpolation of the original 2D STED data on the grid around the centerlines of the mitochondria in the ROIs resulted in straightened mitochondria sections. These straightened sections were placed in a continuous row by adjusting the vertical position of each section so that their centers of mass in the vertical direction are equal.

This also allowed separating the mitochondria sections unambiguously into two sides. If they are aligned in a row that would be an upper and a lower side. Adding up the upper and the lower side in the direction across the mitochondria resulted in two intensity profiles for the two sides of all obtained sections combined. The Pearson correlation coefficient between those two profiles could be computed. An error for the correlation coefficient could be computed by bootstrapping. As a control, the correlation between the two sides was computed with one side shifted along the mitochondria for a small distance (~500 nm) and resulted in no apparent correlation.

The combined, straightened sections of mitochondria predominantly showed a chain of single clusters on each side of the mitochondria. In order to estimate the average distance along the mitochondria between two neighbored clusters for each side of the mitochondria, the following procedure was applied. First, the combined sections were deconvolved with a 2D Gaussian peak of 50 nm FWHM using 10 iterations of the Richardson-Lucy algorithm. Then the clusters were localized by identifying local maxima. The two sides of

the mitochondria were separated and only the position of the local maxima along the mitochondria was noted. The distances between consecutive positions gave the distances between neighbored clusters, where only consecutive positions within the same original section were regarded and the results of both sides of the mitochondria were aggregated. Please note that because of the finite resolution the estimated distance between neighbored clusters is limited to a distance of approximately > 50 nm.

Potassium permanganate fixation of yeast cells, Focused Ion Beam milling combined with Scanning Electron Microscopy (FIB-SEM) and subsequent 3D reconstruction of the cristae morphology

S. cerevisiae cells were grown to the early exponential growth phase ($OD_{600\ nm}$ = 0.4 - 0.7) in liquid medium containing galactose as the sole carbon source and harvested by centrifugation. Cells were fixed utilizing 2 % glutaraldehyde in 0.1 M sodium cacodylate buffer at pH 7.4 (RT, 30 min). Subsequently, the cells were pelleted and postfixed with 1.5 % potassium permanganate (RT, 2 h). After that the cells were washed with distilled water (3x) and resuspended in 2 % agarose. The resulting agarose block was carefully partitioned, stained with 1 % uranyl acetate, dehydrated consecutively by increasing ethanol concentrations and embedded in Agar 100 resin (Agar Scientific, Essex, UK).

In preparation for FIB-SEM imaging, the embedded cells were mounted on aluminium SEM stubs (diameter 12 mm) and coated with ~8 nm of Platinum (Quorum Q150T ES, Lewes, UK). The Zeiss Crossbeam 540 system in combination with the Atlas5 software (Carl Zeiss, Oberkochen, Germany) was utilized for FIB-SEM imaging. Consecutive sections of 5 nm were removed by FIB milling (via propelling Gallium ions at the sample surface; probe current: 700 pA). Image acquisition was performed at 1.5 kV and 600 pA using an ESB (back-scattered electron) detector, with the ESB grid set at -1200 V. The resulting data set was segmented semiautomatically and reconstructed using the software package IMOD (http://bio3d.colorado.edu/imod/) and Amira for Life Sciences (Thermo Fisher Scientific) software.

Transmission electron microscopy of human fibroblasts

For transmission electron microscopy, HDFa cells were grown on Aclar discs (Plano, Wetzlar, Germany) to a confluence of ~50 % and fixed with prewarmed 2.5 % glutaraldehyde in 0.1 M cacodylate buffer (pH 7.4) (RT, 1h). Fixation was completed overnight (4 °C). After washing three times with 0.1 M cacodylate buffer the cells were stained in 1 % (w/v) osmium tetroxide in 0.1 M cacodylate buffer (RT, 1h).

The cells were washed with distilled water (3 times each for 5 min) and stained en-bloc in aqueous 1 % (w/v) uranyl acetate in the dark (RT, 30 min). After dehydration in an ethanol series of 30, 50, 70 and 100 % (three times each for 5 min) with a final dehydration step in propylene oxide (5 min) the cells were embedded in Agar 100 epoxy resin. Sections of 50 nm thickness were recorded on a Philips CM120 transmission electron microscope at 15000× magnification with a TVIPS 2k × 2k slow-scan CCD camera.

Figure S1

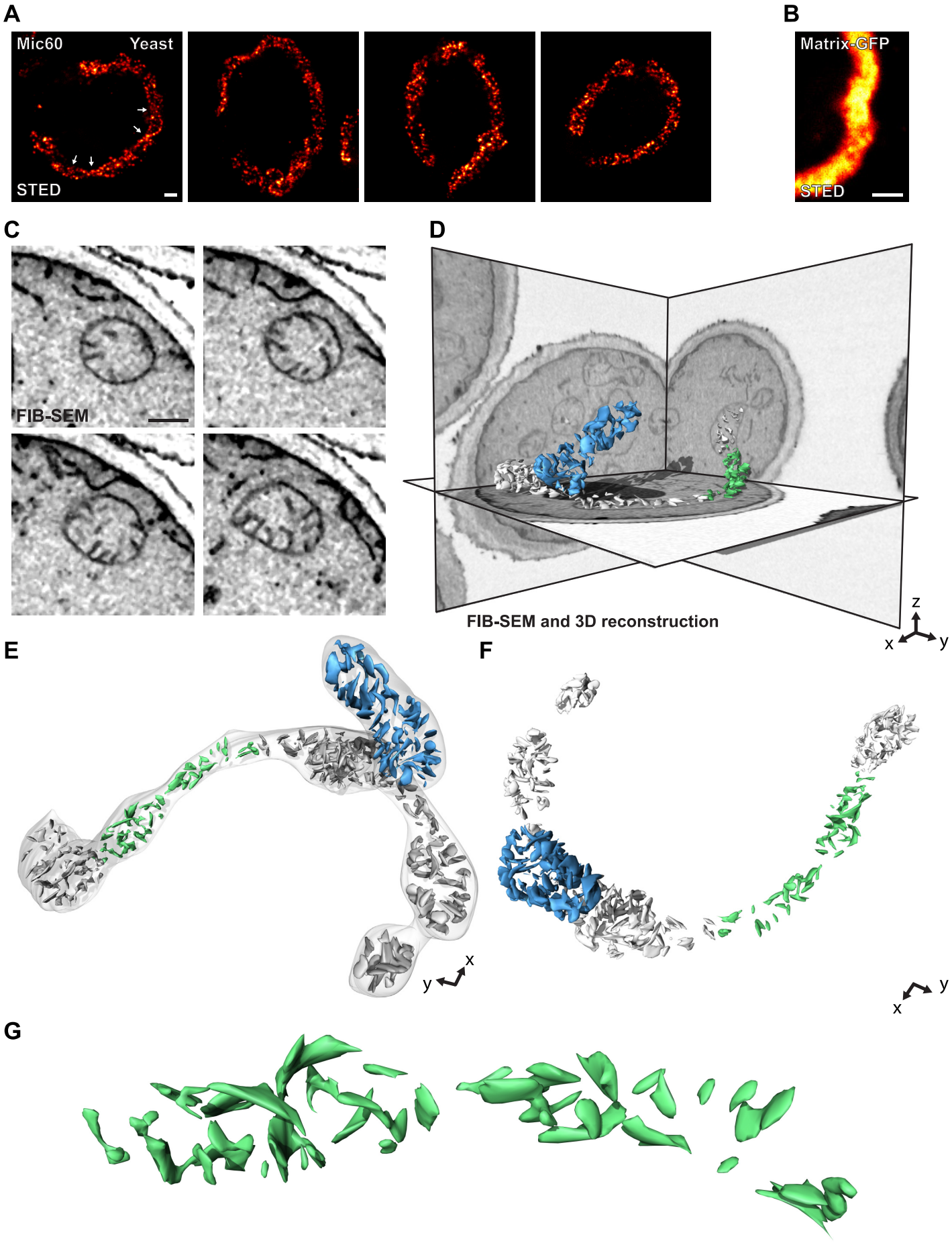
A
Mic60
Yeast
STED
B
Matrix-GFP
STED
C
FIB-SEM
D
FIB-SEM and 3D reconstruction
z
x
y
E
y
x
F
x
y
G

Fig. S1. Mic60 and the cristae are often arranged in a helical pattern in budding yeast mitochondria.

A. STED nanoscopy of entire yeast cells expressing Mic60-GFP fusion proteins. Cells were labeled with a GFP-specific antiserum.

B. STED nanoscopy of matrix targeted GFP in the mitochondria of *S. cerevisiae*. Cells were labeled with a GFP-specific antiserum.

C. Slices of a mitochondrion from wild type budding yeast recorded by FIB-SEM. *S. cerevisiae* cells grown with galactose as the sole carbon source to the early logarithmical phase at 30 °C were chemically fixed and analyzed by FIB-SEM. Shown are four slices of the mitochondrion which is depicted in Figs. 1 C,D.

D. Ortho slice view and part of the reconstructed cristae of the cell shown in C. Images show a FIB-SEM stack with one yeast cell at its center and highlight the cellular position of the mitochondrion depicted in Figs. 1 C,D.

E-G. Different views on parts of the reconstructed cristae of the cell shown in C. The part used for the rendition shown in Figs. 1 C,D is depicted in blue.

With the exception of contrast stretching no further image processing was applied to the STED images. Scale bars: 400 nm (A, B), 150 nm (C, G).

Figure S2

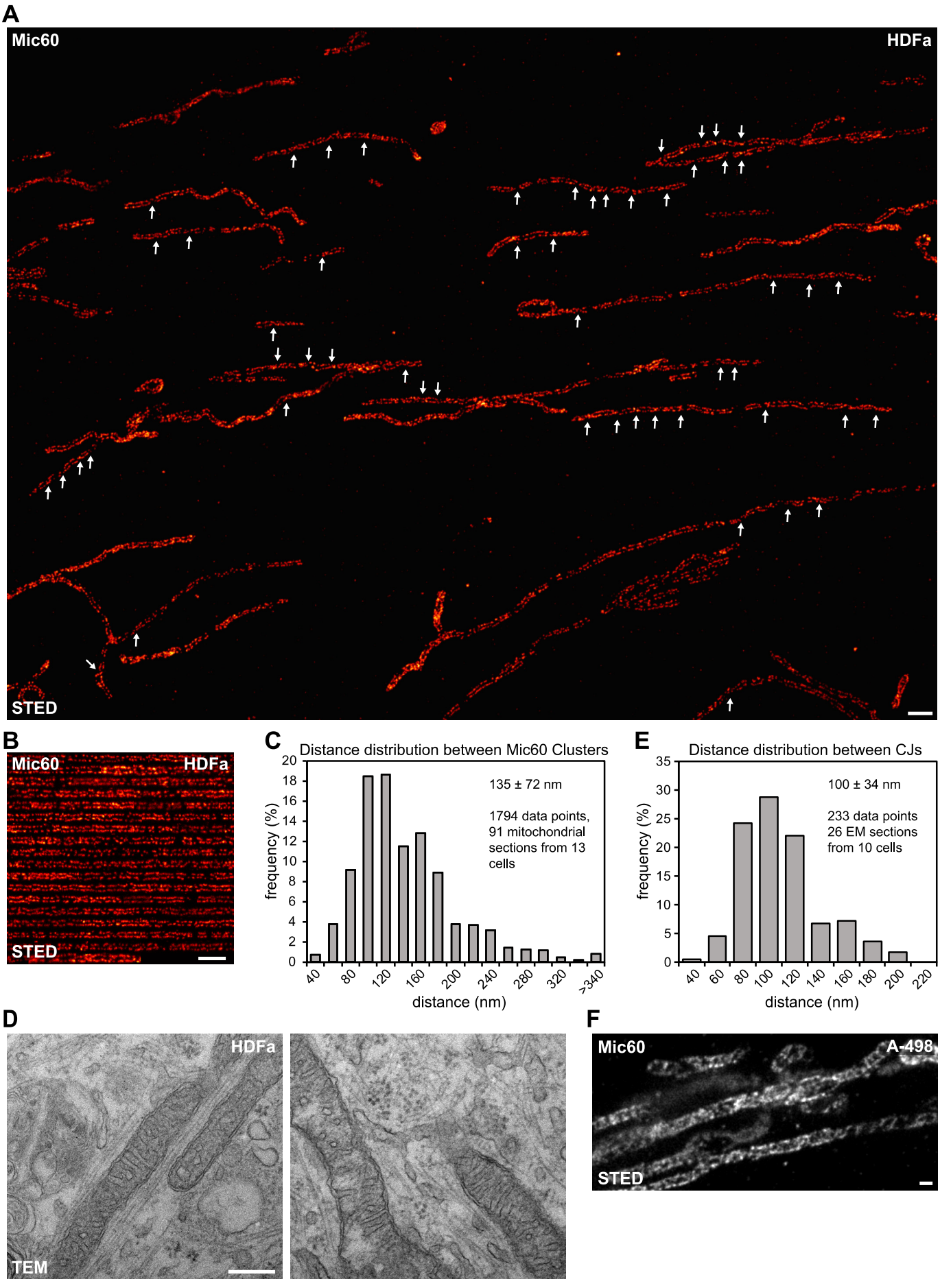
A
Mic60
HDFa
STED
B
Mic60
HDFa
STED
C
Distance distribution between Mic60 Clusters
135 ± 72 nm
1794 data points,
91 mitochondrial
sections from 13
cells
frequency (%)
distance (nm)
E
Distance distribution between CJs
100 ± 34 nm
233 data points
26 EM sections
from 10 cells
frequency (%)
distance (nm)
D
HDFa
TEM
F
Mic60
A-498
STED

Fig. S2. Mic60 exhibits a scaffold-like distribution in the mitochondria of mammalian cells

A. STED nanoscopy of Mic60 in HDFas. Cells were labeled with a Mic60 antiserum and recorded by STED nanoscopy. Mitochondrial segments showing twisted Mic60 patterns are marked by arrows.

B-C. HDFa cells were labeled with a Mic60 antiserum and recorded by STED nanoscopy. The labeled mitochondria were automatically identified and straightened *in silico* (B). Subsequently, the distance distribution between Mic60 clusters along one side of the mitochondrial tubules were determined (C).

D-E. Measurement of the distance distribution of cristae junctions along one side of the mitochondrial tubules in HDFa cells (E) based TEM images (D).

F. Spatial distribution of Mic60 in mitochondria from A-498 cells. Human A-498 cells were labeled with a specific antiserum against Mic60 and recorded by STED nanoscopy. Shown are raw data.

With the exception of contrast stretching no further image processing was applied. Scale bars: 1 µm (A, B); 200 nm (D, F).

Figure S3

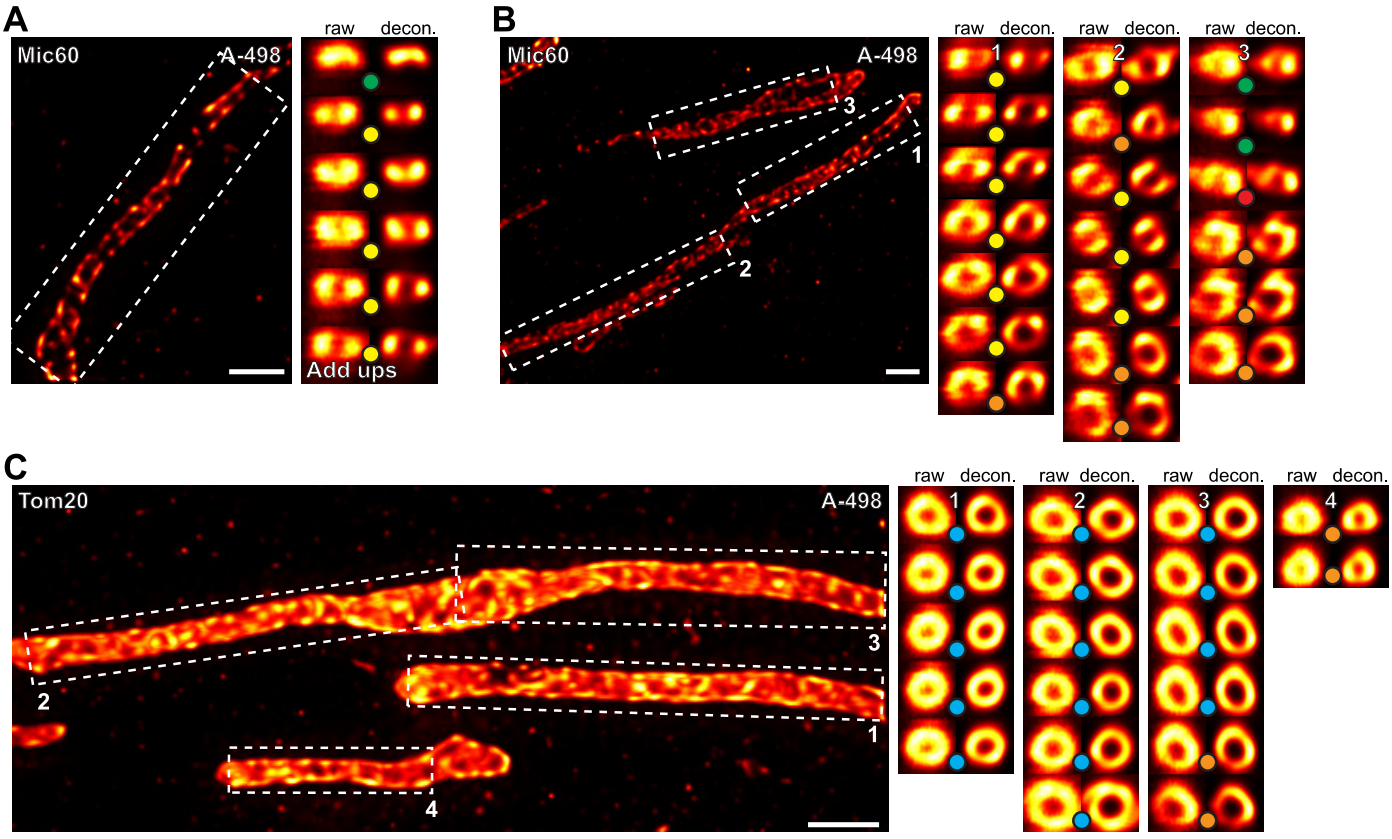

D

Protein distribution in add ups

Protein distribution shapes

ring (homogeneous)	
round filled spot (no hole)	
elongated spot (no hole)	
two opposing spots	
U shape (ring with a gap)	
irregular (none of the above)	

E

Tom20 [%]
55.7
10.4
8.0
2.0
19.9
4.0
n = 201

F

Mic60 [%]
6.6
15.1
18.8
17.1
37.0
5.7
n = 351

Fig. S3. Mic60 is localized in opposing distribution bands in human mitochondria

A-B. 3D STED nanoscopy of Mic60 in A-498 cells. Left: One optical section of a 3D STED image of mitochondria of A-498 cells decorated for Mic60. Right: Longitudinally added Mic60 fluorescence signals from the mitochondrial segments as indicated in the corresponding STED image. Each segment covers 1.5 µm. To add the fluorescence intensities, the straightened tubules were automatically segmented into parts of 1.5 µm, each overlapping with the next by 750 nm. Subsequently, the fluorescence signal of each segment along the longitudinal mitochondrial axis (over 1.5 µm) was added up. Segments were manually assigned to different categories. The assigned categories are indicated by the color-coded spheres.

C. 3D STED nanoscopy of Tom20 in A-498 cells. The images were processed and analyzed as detailed for A-B.

D. Explanation of the color coding used for assignment. Shown are representative images for each category.

E-F. Statistical evaluation of segments with added up fluorescence signals. Analyzed were 201 Tom20, and 351 Mic60 segments. Scale bars: 1 µm (A-C).

Figure S4

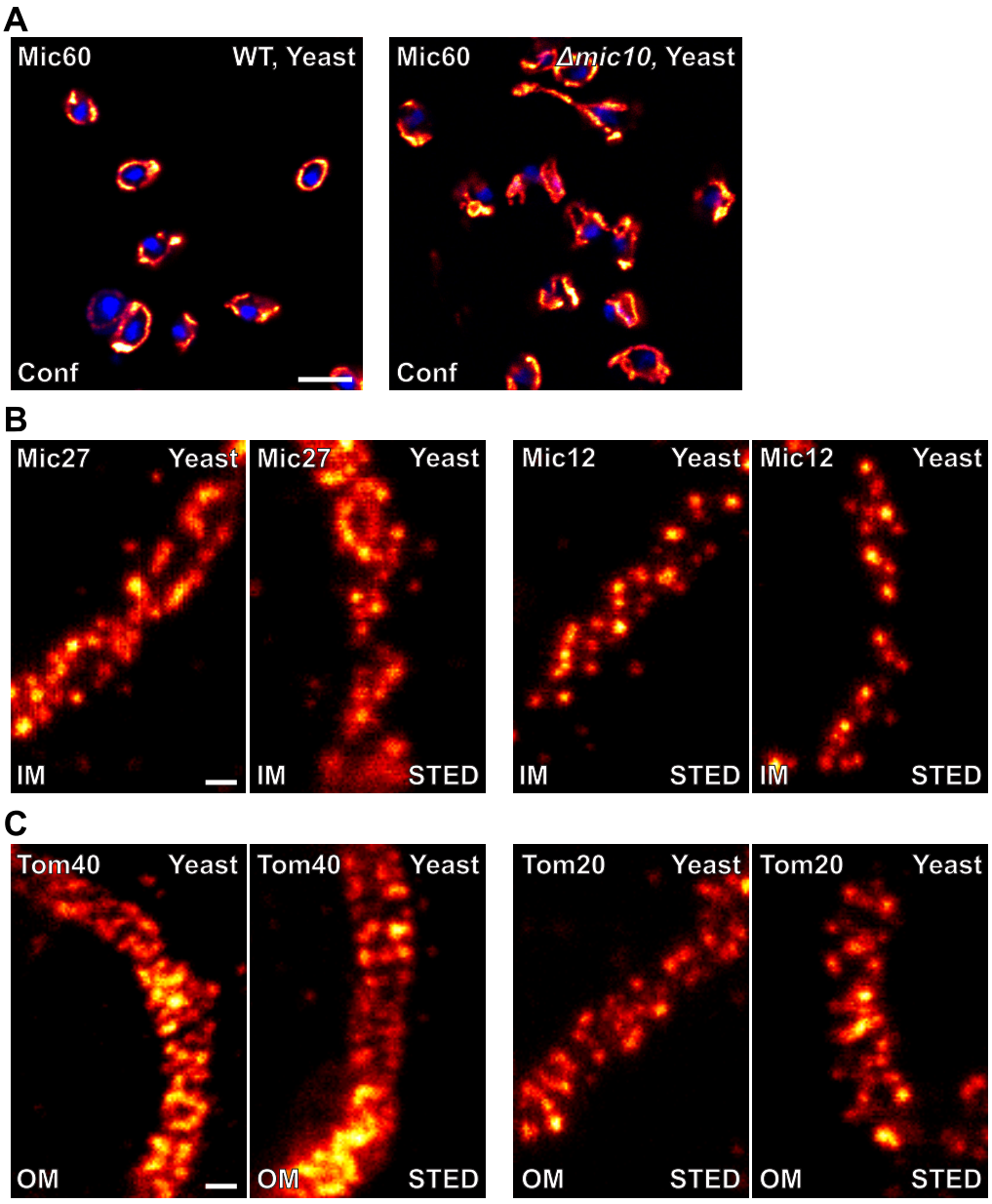
A
Mic60
WT, Yeast
Conf
Mic60
Δmic10, Yeast
Conf
B
Mic27
Yeast
IM
Mic27
Yeast
IM
STED
Mic12
Yeast
IM
Mic12
Yeast
IM
STED
C
Tom40
Yeast
OM
Tom40
Yeast
OM
STED
Tom20
Yeast
OM
Tom20
Yeast
OM
STED

Fig. S4. Nanoscale distribution of yeast mitochondrial inner and outer membrane proteins.

A. Confocal overview images of Mic60-GFP in wild type and Δ*mic10* cells labeled with a GFP-specific antiserum.

B. Localization of integral membrane proteins of the mitochondrial inner membrane (IM) recorded by single-color STED nanoscopy. Yeast strains expressing GFP-tagged versions of the indicated proteins from their native loci were labeled using a GFP-specific antiserum. Shown are exemplary images.

C. Localization of integral membrane proteins of the mitochondrial outer membrane (OM) recorded by single-color STED nanoscopy. Tom40 was labeled using a specific antiserum. Yeast strains expressing GFP-tagged versions of the indicated proteins from their native loci were labeled using a GFP-specific antiserum. Shown are exemplary images.

With the exception of contrast stretching no further image processing was applied. Scale bars: 5 µm (A), 200 nm (B, C).

Table S1. Yeast strains generated for this study

Strain	Tagged Protein	Genotype
Mic60-GFP (W303)	Mic60-GFP	*MATa; ura3-1; trp1Δ 2; leu2-3, 112; his3-11, 15; ade2-1; can1-100; MIC60GFP::HIS3*
Mic60-GFP; Δmic10 (W303)	Mic10-K.O.; Mic60-GFP	*MATa; ura3-1; trp1Δ 2; leu2-3, 112; his3-11, 15; ade2-1; can1-100; MIC60GFP::HIS3; mic10::kanMX*
Mic27-GFP (W303)	Mic27-GFP	*MATa; ura3-1; trp1Δ 2; leu2-3, 112; his3-11, 15; ade2-1; can1-100; MIC27GFP::HIS3*
Mic12-GFP (W303)	Mic12_GFP	*MATa; ura3-1; trp1Δ 2; leu2-3, 112; his3-11, 15; ade2-1; can1-100; MIC60GFP::HIS3*
Tom20-GFP (W303)	Tom20-GFP	*MATa; ura3-1; trp1Δ 2; leu2-3, 112; his3-11, 15; ade2-1; can1-100; TOM20GFP::HIS3*
Om14-GFP (W303)	Om14-GFP	*MATa; ura3-1; trp1Δ 2; leu2-3, 112; his3-11, 15; ade2-1; can1-100; OM14GFP::HIS3*

Table S2. Primer for genomic tagging

Gene/ ORF	Primer name	Primer sequence
MIC60	Mic60_S3	GAAGTCCAGCGCCTGGTAGAGATTCTTGACTGTGAAATAAGGACGTTGCGTACGC TGCAGGTCGAC
MIC60	Mic60_S2	GGAAATTGAGGTGTAATGACGTACATCTCTTTTCTCTTTGTATTATTCTTTCAATCG ATGAATTCGAGCTCG
MIC27	Mic27_S3	CAAAAAAATATAAGGTATGCAAGGGAACAGCTTTATGAAAAGTTGGAGCAAGCA CGTACGCTGCAGGTCGAC
MIC27	Mic27_S2	CTTACTATGGACATGATAATGAACAAAAAAAGATATCCGCTTGATATCAATCGATG AATTCGAGCTCG
MIC12	Mic12_S3	GAACAGATAAGAAACTCTGTCGATTGGATCTACTCCTGGGGTAAGAATCGTACGC TGCAGGTCGAC
MIC12	Mic12_S2	GGTTATATACATGAGGATGTTCGTTACAGTAGGAGAAATAGAAAGCTCGCTAATC GATGAATTCGAGCTCG
TOM20	Tom20_S3	GCAAGGCCGAATCTGATGCGGTTGCTGAAGCTAACGATATCGATGACCGTACGCT GCAGGTCGAC
TOM20	Tom20_S2	GAGTAAAAGAAACAAAAACGGAGAAAAAAAGCAAGCAAAATGTTACTCTCAATC GATGAATTCGAGCTCG
OM14	Om14_S3	CTGGACGGTATAATTTCAAAGAAATACTACTCCAGATACGACAAGAAACGTACGC TGCAGGTCGAC
OM14	Om14_S2	GTGAGTGTGTGAGTGTGTGAAAGGATGTTATTAAATAGTATGTTATTAATCGATG AATTCGAGCTCG

Table S3. Primer for targeted gene disruption

Gene/ ORF	Primer name	Primer sequence
MIC10	Mic10_A	AGCTAGGTGACATGTATACTGGAGC
MIC10	Mic10_D	GGAAGAGAACAAAGTTACAAGTGGA

Table S4. Primary antibodies used in this study

Antibody	Host species	Depositor/ Supplier	Catalog number	Lot number
Anti-GFP	Rabbit	Abcam	ab6556	GR292567-1
Anti-Porin [16G9E6BC4]	Mouse	MitoSciences (Abcam)	MSA08 (ab110326)	FKASHK
Anti-Mic10	Rabbit	Peter Rehling, Georg-August-University Göttingen, Germany	-	-
Anti-Tom40	Rabbit	Peter Rehling, Georg-August-University Göttingen, Germany	-	-
Anti-Mic60	Rabbit	Proteintech	10179-1-AP	2
Anti-Tom20	Rabbit	Santa Cruz Biotechnology	sc-11415	G0811
Anti-Tom20 [EPR15581]	Rabbit	Abcam	ab186734	GR219533-17
Anti-Tom22	Mouse	Miltenyi Biotec, Bergisch Gladbach, Germany	-	-

Movie S1. **Cristae are often arranged in a helical pattern in budding yeast mitochondria.** FIB-SEM recording of a budding yeast cell grown in galactose containing medium. Displayed is an orthoslice moving through the data stack recorded by FIB-SEM. The cristae are rendered in blue, green and white, the outer membrane is displayed in gray.

Movie S2. **3D distribution of Mic60 in human mitochondria.** Visualization of a 3D STED recording of Mic60 in human A-498 cells. Mic60 was labeled with a specific antiserum against Mic60. 3D STED data were deconvolved, contrast stretched and visualized as a 3D volume rendition.

References for SI reference citations

1. Schauss AC, Bewersdorf J, & Jakobs S (2006) Fis1p and Caf4p, but not Mdv1p, determine the polar localization of Dnm1p clusters on the mitochondrial surface. *Journal of Cell Science* 119(15):3098-3106.
2. Janke C, *et al.* (2004) A versatile toolbox for PCR-based tagging of yeast genes: new fluorescent proteins, more markers and promoter substitution cassettes. *Yeast* 21(11):947-962.